Avocado seed powder: characterization and its application for crystal violet dye removal from aqueous solutions

Alexandre Bazzo[a], Matthew A. Adebayo[b], Silvio L.P. Dias[a,*], Eder C. Lima[a],
Júlio C.P. Vaghetti[a], Eduardo R. de Oliveira[a], Anderson J.B. Leite[a], Flávio A. Pavan[c]

[a]Institute of Chemistry, Federal University of Rio Grande do Sul (UFRGS), Av. Bento Gonçalves 9500, P.O. Box 15003, ZIP 91501-970, Porto Alegre, RS, Brazil, email: alexandre.bazzo@ufrgs.br (A. Bazzo), Tel. +55 51 3308 7175; Fax: + 55 51 3308 7304; emails: silviol@ufrgs.br, silvio@iq.ufrgs.br (S.L.P. Dias), profederlima@gmail.com (E.C. Lima), juliovaghetti@gmail.com (J.C.P. Vaguetti), eroliv@iq.ufrgs.br (E.R. de Oliveira), barcellos2903@gmail.com (A.J.B. Leite)
[b]Department of Chemistry, Federal University of Agriculture, PMB 2240, Abeokuta, Ogun State, Nigeria, email: adebayomao@gmail.com
[c]Institute of Chemistry, Federal University of Pampa (UNIPAMPA), Bagé, RS, Brazil, email: flavio.pavan@unipampa.edu.br

Received 9 January 2015; Accepted 14 July 2015

ABSTRACT

This study presents removal of crystal violet (CV) dye from aqueous solutions using solid food waste, avocado kernel seed powder (ASP). ASP was used in the native form for biosorption study. The effects of different experimental conditions such as pH of the solution, initial dye concentration, contact time, and temperature were investigated using batch study. Maximum removal of CV (95.9 mg g^{-1}) by ASP (100 mg) was observed at pH 7 and 55°C. The kinetics data were evaluated using pseudo-first-order, pseudo-second-order, and general-order kinetic adsorption models. The general-order kinetic adsorption model gave the best description of the biosorption kinetic of CV onto ASP biosorbent. Similarly, the intraparticle diffusion plots showed three linear portions during biosorption process. Freundlich, Langmuir, and Liu models were used to analyze the isothermal data; Liu equilibrium model gave the best fit of the isothermal data of CV biosorption onto ASP. The calculations from thermodynamic studies showed that CV biosorption onto ASP was an exothermic process and a feasible process. The combined data showed that avocado seed powder could be efficiently utilized for the treatment of dyes-rich wastewaters.

Keywords: Avocado seed; Adsorption; Equilibrium; Kinetic; Crystal violet

1. Introduction

Industrial developments, as a result of population growth and urbanization, have led to an increment in environmental pollution. A number of industries such as textile industries utilize dyes for coloring their products. It is imperative to treat the industrial waste effluents emanating from textile industries before being released into the environment [1–3]. Synthetic dyes and pigments constitute nuisance to the environment. Presence of dyes in the aquatic environment does not only cause offensive coloration, but also affects plants growth and development by impeding their photosynthetic rate [4,5]. Synthetic dyes are non-biodegradable, toxic, mutagenic and carcinogenic, and

*Corresponding author.

can also induce skin cancer and allergies even at low concentrations [6,7]. To alleviate environmental damages and improve water quality, a lot of techniques have been recently employed to remove hazardous dyes from waste effluents [8,9].

Techniques such as electrochemical [10], biological treatment [9], solvent extraction [11], oxidation [12], and adsorption [13] have been used to remove dyes from aqueous effluents. However, the most preferred method for wastewater treatment is the adsorption technique because of its simplicity, rapidness, effectiveness, cheapness, and availability of low-cost adsorbents [14–16]. Activated carbons have been widely used for treatment of industrial wastewaters [17,18], but the usage of activated carbons has some limitations such as the cost of producing activated carbon, industrial scale application, regeneration difficulty and reduction in adsorption efficiency of regenerated activated carbon [19,20]. Attention has been shifted to the usage of eco-friendly and low-cost materials [21,22]. These materials possess high carbon content, but low inorganic content. They are obtainable from variety of agricultural by-products that are cheap, abundant, and nontoxic [1,15,21,22] and can be utilized as alternative biosorbents for the removal of several dyes from aqueous solutions.

Fruit husks, fruit seeds, and fruit peel, among others are agricultural wastes that can be used as biosorbents in their native forms [23]. The kernel of avocado (*Persea americana*), which is discarded in the garbage after consumption, is about 10–13% of the fruit [23]. At present, Brazil occupies the seventh position in the world in the production of avocado—producing 152,181 tons of avocado [24]. The current production of avocado in Brazil generates *ca* 15.2–19.8 tons of kernel (a waste). Therefore, it is necessary to utilize this waste to avoid environmental problems that may be associated with the decomposition of the waste. Degradation of avocado kernel could result in accumulation of unwanted chemicals and microbial growth. Therefore, the use of avocado kernel for wastewater decontamination (removal of dyes) is economical and eco-friendly.

Crystal violet (CV) is used to add color to paper, and it is a component of inks for printing and pens [21]. Also, it is used to add color to products such as fertilizers, anti-freezes, detergents, and leather [22]. CV is used as histological stain, particularly in Gram's method for classifying bacteria [21,22]. Due to its usage in different industrial applications, various adsorbents have been used to remove CV from aqueous solutions [21,22,25–34].

Based on the context of using biomass as biosorbent and that there is a need to remove dyes from aqueous effluents, the use of avocado seeds powder (ASP) as biosorbent for removal of CV dye from aqueous solutions is proposed in this study.

2. Materials and methods

2.1. Solutions and reagents

Analytical grade reagents were used throughout this study. Deionized water was used to prepare all experimental solutions. The initial pH of each solution was adjusted with a 0.10 mol L^{-1} NaOH, a 0.10 mol L^{-1} HCl, or both using a pH-meter (Digimed Model DM 20, Brazil). All experiments were carried out in triplicate.

The analytical grade CV, a cationic dye, (C.I. Basic Violet 3; C.I. 42555; molecular formula $C_{25}H_{30}N_3Cl$; 407.99 g mol^{-1}; λ_{max} 583 nm) was purchased from Sigma Chemical Co., USA. The structural and optimized three-dimensional formulae of CV are shown in Fig. 1. The stock solution (2,000.0 mg L^{-1}) was prepared by weighing and dissolving an accurate mass of the dye in deionized water. The working solutions were prepared by diluting the stock solution of the dye.

2.2. Biosorbent characterization

Avocado fruits (*P. americana*) were purchased from a local market. The seeds of fresh avocado fruits were removed manually. The collected fruits were washed with tap water to remove dirt, then deionized water, and dried in an oven at 75°C for 24 h. Afterward, the seeds were crushed and sieved through a 250-μm sieve to obtain ASP. The ASP was stored in a glass bottle until use.

The specific surface area of ASP was determined using the Brunauer, Emmett, and Teller (BET) multi-point model, obtained by the N$_2$ adsorption technique using a Tristar Krypton 3020 Micromeritics equipment. Prior analysis, a 200.0 mg of ASP was degassed at 150°C for 3 h in a vacuum. The N$_2$ isotherms were carried out at −196°C [35].

Point zero charge (pH$_{zpc}$) of the biosorbent was determined using a reported procedure [15]: a 20.00 mL of 0.050 mol L^{-1} NaCl solution was added to different 50-mL Falcon tubes containing a 50.0 mg of the adsorbent, and were capped immediately. The pH (pH$_i$) values of the solutions were adjusted from 1.0 to 9.0 using a 0.10 mol L^{-1} of HCl and or 0.10 mol L^{-1} NaOH. The suspensions were stirred and equilibrated in a thermostatic shaker at 25°C for 48 h. Thereafter, the suspensions were centrifuged at 10,000 rpm for 10 min. The pH$_i$ of the solutions without biosorbent
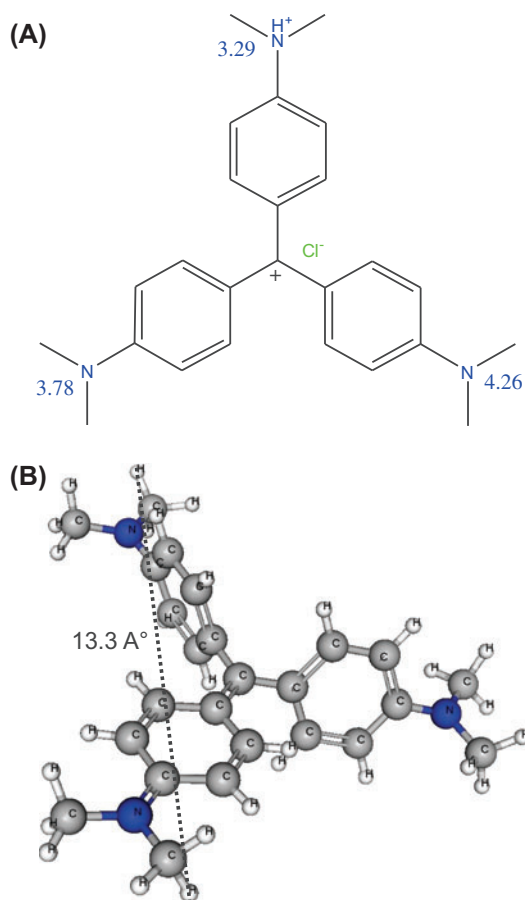
(A)

(B)

13.3 A°

Fig. 1. (A) Structural formula of CV dye and pK_a values of each group and (B) optimized three-dimensional structural formula of CV dye. The physicochemical properties of the molecule were calculated using MarvinSketch (version 14.9.22.0). Van der Waals surface area = 585.65 A^2 (pH 6.00–14.00); polar surface area = 9.49 A^2 (pH 6.00–14.00); dipole moment = 82.57 Debye.

and pH_f of the supernatant after contact with the biosorbents were measured and recorded. The value of pH_{pzc} is the point where the plot of ΔpH ($pH_f - pH_i$) vs. pH_i crosses a line equal to zero [15].

The functional groups of ASP were assessed using Fourier transform infrared spectroscopy (FTIR) (Shimadzu Spectrometer, IR Prestige 21, Kyoto, Japan). For FTIR analysis, a 10.0 mg of ASP and a 100.0 mg of KBr were dried at 120°C for 8 h, stored in capped flasks and kept in a desiccator before FTIR analysis. The spectra were obtained with a resolution of 4 cm^{-1} with 100 cumulative scans.

Scanning electron microscopy (SEM) (JEOL electron microscope, model JSM 5800, with working voltage 10 kV at 350–400× magnification) was used to probe the surface morphology of native ASP.

Thermogravimetric (TGA) and derivative thermogravimetric (DTG) curves were obtained on a TA Instruments, model SDT using the following experimental conditions: initial temperature, 25°C; final temperature, 850°C; mass of biosorbent, 3.00–10.00 mg; heating rate of 10°C min^{-1} and nitrogen flow of 100 mL min^{-1} [36].

2.3. Batch biosorption study

The optimizations of experimental parameters for biosorption of CV by ASP were performed using a 25.0 mL of CV solution (initial concentration of 25.0 mg L^{-1}), contact time (3.0–360.0 min), biosorbent dosage (100 mg/25.0 mL), pH values (2.0–10.0), and temperature (15–55°C). For biosorption equilibrium studies, a fixed amount of ASP (100.0 mg) was placed in different 50.0-mL flat Falcon tubes containing 25.0 mL of dye solutions. After equilibrium was reached, each of systems was centrifuged to separate the biosorbent from the liquid phase, and the unadsorbed dye in the solution was determined using a UV–vis spectrophotometer (T90 + PG Instruments spectrophotometer) with 1.0 cm path length cell. Absorbance values were determined at a maximum wavelength (λ_{max}) of 583 nm of CV.

The amount of dye removed by ASP was evaluated using Eq. (1), while the corresponding percentage of removal was calculated using Eq. (2).

$$q = \frac{(C_o - C_f)}{m} \cdot V \tag{1}$$

$$\% \text{ Removal} = 100 \times \frac{(C_o - C_f)}{C_o} \tag{2}$$

where q is the amount of dye removed by the biosorbent (mg g^{-1}), it is also known as biosorption capacity; C_o is the initial CV concentration in contact with the biosorbent (mg L^{-1}); C_e is the CV concentration (mg L^{-1}) after the batch biosorption; m is the mass of biosorbent (g) and V is the volume of dye (L) in contact with the biosorbent.

2.4. Quality assurance and statistical evaluation of models

To ensure that the experimental data are reproducible, all experiments were carried out in triplicate. The relative standard deviations of all measurements were <5% [37]. Blanks were run in parallel and corrected when necessary [37].

The CV solutions were stored in glass bottles, which were precleaned by immersing in 1.4 mol L^{-1}

HNO_3 for 24 h [37], rinsing with deionized water, drying, and storing them in a closed cabinet.

Standard dye solutions (1.00–12.0 mg L^{-1}), in parallel with a blank (aqueous solution, which is a function of pH of the dye solution being measured), were used for calibration. The linear analytical calibration curve was performed on the UV–Win software of the T90 + PG Instruments spectrometer. All analytical measurements were carried out in triplicate, and the precision of the standards was better than 3% ($n = 3$). The detection limit of CV dye was 0.020 mg L^{-1} with a signal/noise ratio of three [38]. A 5.00 mg L^{-1} of standard dye solution was used as a quality control after every five determinations to ensure accuracy of the CV dye solutions [37].

To fit both kinetic and equilibrium data, the data were subjected to nonlinear methods with successive interactions calculated by the Levenberg–Marquardt method. Similarly, interactions were computed using Simplex method based on the nonlinear fitting facilities of the Microcal Origin 9.0 software. The fitness of each model was evaluated using a determination coefficient (R^2), an adjusted determination coefficient (R_{adj}^2) and the Function error (F_{error}) [39,40]. F_{error} is a measure of the differences between the theoretical and experimental amounts of dye adsorbed. Eqs. (3)–(5) show the mathematical relationship of R^2, R_{adj}^2 and SD, respectively.

$$R^2 = \left(\frac{\sum_i^n \left(q_{i,exp} - \bar{q}_{exp} \right)^2 - \sum_i^n \left(q_{i,exp} - q_{i,model} \right)^2}{\sum_i^n \left(q_{i,exp} - \bar{q}_{exp} \right)^2} \right) \quad (3)$$

$$R_{adj}^2 = 1 - \left(1 - R^2 \right) \cdot \left(\frac{n-1}{n-p-1} \right) \quad (4)$$

$$F_{error} = \sqrt{ \left(\frac{1}{n-p} \right) \cdot \sum_i^n \left(q_{i,exp} - q_{i,model} \right)^2 } \quad (5)$$

In Eqs. (3)–(5), $q_{i,model}$ is the individual theoretical q value predicted by the model; $q_{i,exp}$ is the individual experimental q value; $\bar{q}_{exp}$ is the average of experimental q values; n is the number of experiments; p is the number of parameters in the fitting model [39,40].

2.5. Kinetic models

Rate law's exponents of chemical reactions are mostly independent of the coefficients of chemical equations, but related sometimes. It means that the order of a chemical reaction depends on the experimental data. To establish the general rate law equation

for biosorption, the biosorption process on the surface of biosorbent is considered to be the rate-determining step [41,42]. Attention is now focused on the change in the effective number of active sites at the surface of biosorbent during biosorption instead of concentration of adsorbate in bulk solution. Applying reaction rate law to Eq. (6) gives biosorption rate expression.

$$\frac{dq}{dt} = k_N (q_e - q_t)^n \quad (6)$$

where k_N is the rate constant; q_e is the amount of adsorbate adsorbed by adsorbent at equilibrium; q_t is the amount of adsorbate adsorbed by adsorbent at a given time, t; n is the order of biosorption with respect to the effective concentration of the biosorption active sites present on the surface of biosorbent. Application of universal rate law to biosorption process led to Eq. (6), which can be used without assumptions. Theoretically, the exponent n in Eq. (6) can be an integer or non-integer rational number [41,42].

Eq. (7) describes the number of the active sites (θ_t) available on the surface of biosorbent for biosorption [41,42].

$$\theta_t = 1 - \frac{q_t}{q_e} \quad (7)$$

Eq. (8) describes the relationship between the variable (θ_t) and rates of biosorption.

$$\frac{d\theta_t}{dt} = -k\theta_t^n \quad (8)$$

where $k = k_N (q_e)^{n-1}$.

For an unadsorbed biosorbent $\theta_t = 1$, which decreases during biosorption process. θ_t approaches a fixed value when biosorption process reaches equilibrium. For a saturated biosorbent, $\theta_t = 0$ [42].

Eq. (8) gives Eq. (9).

$$\int_1^\theta \frac{d\theta_t}{\theta_t^n} = -k \int_0^t dt \quad (9)$$

Similarly, Eq. (9) gives Eq. (10).

$$\frac{1}{1-n} \cdot \left[\theta_t^{1-n} - 1 \right] = -kt \quad (10)$$

Eq. (10) gives Eq. (11) on rearrangement.

$$\theta_t = [1 - k(1-n) \cdot t]^{1/1-n} \tag{11}$$

Substituting Eq. (7) into Eq. (11), and put $k = k_N(q_e)^{n-1}$, Eq. (12) is obtained.

$$q_t = q_e - \frac{q_e}{\left[k_N(q_e)^{n-1} \cdot t \cdot (n-1) + 1 \right]^{1/1-n}} \tag{12}$$

Eq. (12) is the general-order kinetic equation of biosorption; valid for $n \neq 1$ [42].

A special case of Eq. (8) is the pseudo-first-order kinetic model ($n = 1$) [41,42].

$$\frac{d\theta_t}{dt} = -k \cdot \theta_t^1 \tag{13}$$

Eq. (13) on integration gives Eq. (14).

$$\theta_t = \exp(-k \cdot t) \tag{14}$$

Substitution of Eq. (7) into Eq. (14), and put $k = k_1$ gives pseudo-first-order kinetic model (Eq. (15)).

$$q_t = q_e[1 - \exp(-k_1 \cdot t)] \tag{15}$$

Pseudo-first-order kinetic equation is a special case of general-kinetic model of adsorption.

When $n = 2$, the pseudo-second-order kinetic model is a special case of Eq. (12) [43].

$$q_t = q_e - \frac{q_e}{[k_2(q_e) \cdot t + 1]} \tag{16}$$

Eq. (16) on rearrangement gives Eq. (17).

$$q_t = \frac{q_e^2 k_2 t}{[k_2(q_e) \cdot t + 1]} \tag{17}$$

Eq. (18) is a mathematical expression for the intra-particle diffusion equation [44].

$$q_t = k_{id} \sqrt{t} + C \tag{18}$$

where k_{id} is intraparticle diffusion rate constant (mg g^{-1} h$^{-0.5}$); C is a constant, which is related to the thickness of boundary layer (mg g^{-1}).

Pseudo-first-order (Eq. (15)), pseudo-second-order (Eq. (17)), general-order equation (Eq. (12)), and intraparticle diffusion (Eq. (18)) models were used to evaluate the kinetics of biosorption of the dye on the biosorbent.

2.6. Equilibrium models

The following isotherm models were used to evaluate the equilibrium of biosorption.

Langmuir isotherm model [45].

Eq. (19) shows mathematical relation for Langmuir model.

$$q_e = \frac{Q_{max} \cdot K_L \cdot C_e}{1 + K_L \cdot C_e} \tag{19}$$

where q_e is the amount adsorbate adsorbed at the equilibrium (mg g^{-1}); Q_{max} is the maximum biosorption capacity of the biosorbent (mg g^{-1}); K_L is the Langmuir equilibrium constant (L mg^{-1}); C_e is equilibrium adsorbate concentration (mg L^{-1}).

Freundlich isotherm model [46].

Eq. (20) is a mathematical expression for Freundlich model.

$$q_e = K_F \cdot C_e^{1/n_F} \tag{20}$$

where K_F is the Freundlich equilibrium constant [mg g^{-1} (mg L^{-1})$^{-1/n_F}$]; n_F is a dimensionless exponent of the Freundlich equation.

Liu isotherm model [47].

Eq. (21) shows the Liu isotherm model.

$$q_e = \frac{Q_{max} \cdot (K_g \cdot C_e)^{n_L}}{1 + (K_g \cdot C_e)^{n_L}} \tag{21}$$

where Q_{max} is the maximum biosorption capacity of the biosorbent (mg g^{-1}); K_g is the Liu equilibrium constant (L mg^{-1}); n_L is a dimensionless exponent of the Liu equation; C_e is adsorbate concentration at the equilibrium (mg L^{-1}).

2.7. Simulated dye-house effluents

At pH 7.0, two simulated dye-house effluents that resemble industrial textile effluents were prepared. These effluents contained six representative dyes for fabric colorants and likely secondary chemicals. The concentrations of the effluent components are given in Table 1. Between 10 and 60% [13] of synthetic dyes and almost all the secondary chemicals remain in the spent dye bath, and their compositions undergo

between 5-fold and 30-fold dilutions during consecutive washing and rinsing steps [1,13,15,20,35,36,42,48].

3. Results and discussion

3.1. Characterization of the ASP biosorbent

The N_2 adsorption/desorption curve of ASP gave the following textural properties: superficial area (S_{BET}), 1.75 $m^2 g^{-1}$, and total pore volume, 3.9×10^{-3} $cm^3 g^{-1}$. Fig. 2(A) shows the isotherm of adsorption and desorption of N_2 on ASP. A hysteresis is observed in the biosorbent material at P/P_0 0.7–0.9. This isotherm is classified as type II, which is a characteristic of mesoporous material [49]. Fig. 2(B) presents the pore size distribution of ASP. From this figure it is visible that mesopore region varies from 2.7 to 37 nm. The low surface area of the biosorbent agreed with that of lignin cellulosic materials [1,15,31], but large distribution of the pores in the mesopores region will facilitate biosorption of CV in the ASP pores—CV dye has a maximum longitudinal length of 13.3 Å (1.33 nm) (see Fig. 1).

Fig. 3 shows the thermogravimetric profile of ASP under N_2 atmosphere. From 25.5 to 844.5°C, the final residual mass is 10.9%. Two decomposition peaks (55.7 and 318.5°C) are prominent in DTG curve of ASP. Based on the DTG curve, three regions are present in the TG curve of ASP. A mass loss of 13.9% (25.5–233.2°C) is attributed to water molecules. The humidity of ASP is large compared with inorganic adsorbents [2,14] that possess humidity, however, the
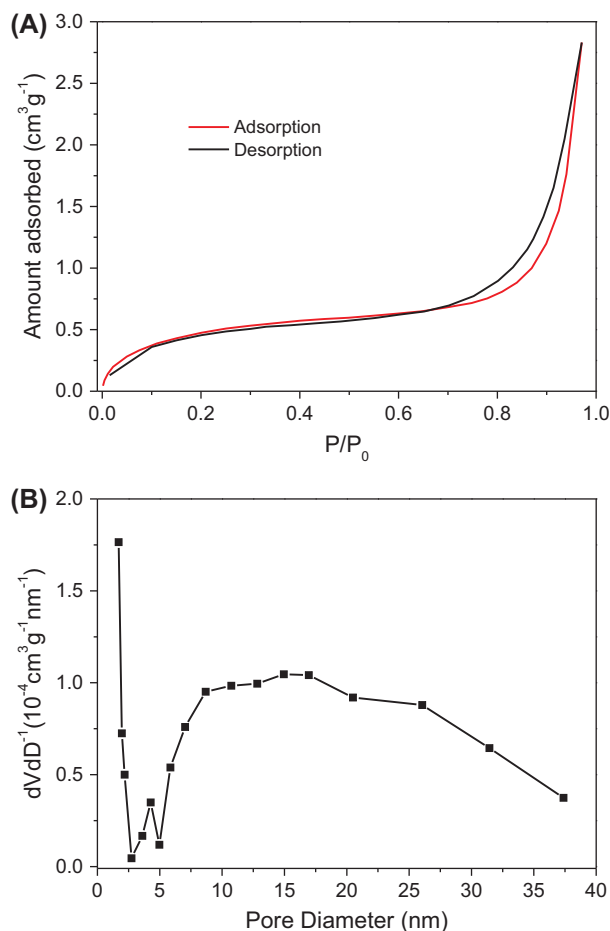
Fig. 2. (A) Isotherm of adsorption and desorption of nitrogen of ASP biosorbent. (B) BJH pore diameter distribution of ASP biosorbent.

Table 1
Chemical composition of the simulated dye-house effluents

	Concentration (mg L^{-1})	
Dyes	Effluent A	Effluent B
Crystal violet (λ_{max} 583 nm)	10.0	20.0
Reactive red 120 (λ_{max} 535 nm)	2.00	5.00
Reactive orange 16 (λ_{max} 489 nm)	2.0	5.00
Cibacron brilliant yellow 3G-P (λ_{max} 402 nm)	2.0	5.00
Remazol brilliant blue (λ_{max} 594 nm)	2.0	5.00
Vilmafix red RR-2B (λ_{max} 505 nm)	2.0	5.00
Auxiliary chemicals		
Na_2SO_4	25.0	25.0
NaCl	25.0	25.0
Na_2CO_3	20.0	20.0
CH_3COONa	50.0	50.0
Sodium dodecyl sulfate (SDS)	50.0	50.0
pH[a]	7.0	7.0

[a]pH of the solution was adjusted with a 0.10 mol L^{-1} HCl, a 0.10 mol L^{-1} NaOH, or both.
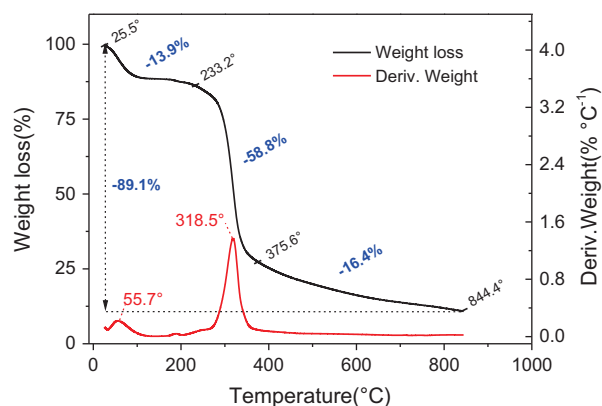
Fig. 3. TGA and DTG curve of ASP biosorbent.

humidity of ASP matches that of lignin-cellulosic materials [13]. A mass loss of 58.8% (233.2–375.6°C), which is assigned to the decomposition of lignin and cellulose, is also observed. Finally, a mass loss of 16.4% (375.6–844.4°C) that could be assigned to degradation of lignin [19,36] is noticed.

Fig. 4 presents the SEM images of ASP. The images show that ASP fiber has roughness similar to that of an open flower. The fiber also contains some spherical lignin-cellulosic material. Generally, the SEM image of ASP is identical to that of lignin-cellulosic material [15,42].

For the identification of functional groups possessed by ASP and the groups that are responsible for biosorption of CV dye, FTIR was used. Fig. 5 shows the FTIR spectrum of ASP. The spectrum was recorded between 4,000 and 400 cm^{-1}. The following bands are observed in the FTIR spectrum of ASP: strong band at 3,287 cm^{-1} that is assigned to O–H group [15,36]; a sharp band at 2,920 cm^{-1} is given to CH_2 stretch [15]; a band at 1,732 cm^{-1} is allocated to carbonyl groups of carboxylic acid [15]; a sharp band at 1,586 cm^{-1} is assigned to asymmetric CO_2 stretch; small bands at 1,522 and 1,439 cm^{-1} are assigned to ring modes of aromatic ring [15,36]; a small band at 1,361 cm^{-1} is assigned to OH bending [15,36]; a band at 1,290 cm^{-1} is assigned to C–O stretch of phenols; and a band at 1,014 cm^{-1} is assigned to C–O stretch of cellulose [15,36]. It means that the major functional groups of ASP are: O–H (alcohols and phenols), C=O of carboxylic acids, aromatic rings, C–O (alcohols and phenols), and C–H (aromatics and aliphatic chains).

3.2. Influence of initial pH on the sorption capacity of ASP

The initial pH of the adsorbate solution is one of the most important parameters that influence the biosorption of a dye on a biosorbent [13–15,36]. The
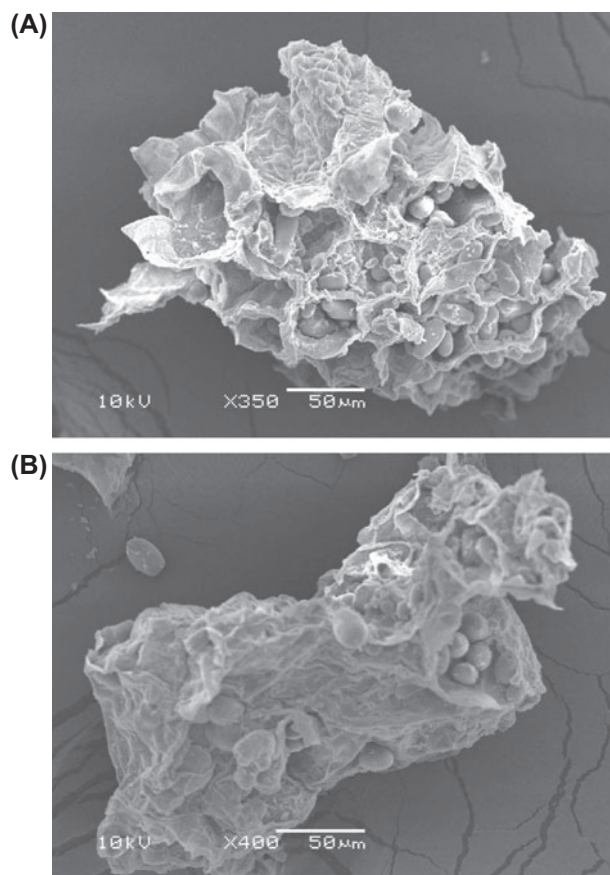

Fig. 4. SEM images of ASP biosorbent. (A) magnification 350× and (B) magnification 400×.
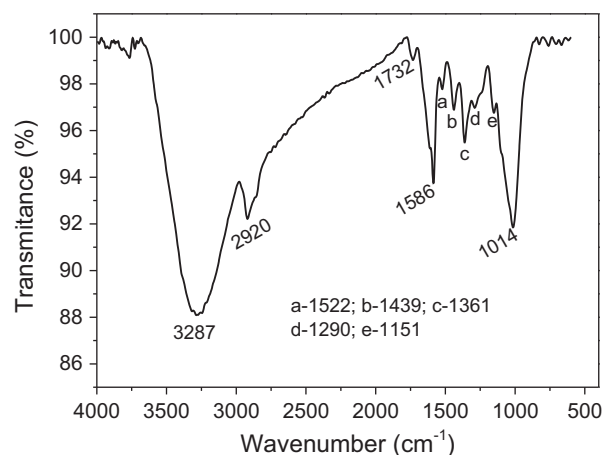

Fig. 5. FTIR spectrum of ASP biosorbent. Numbers inside the graph corresponds to FTIR bands expressed in cm^{-1}.

functional (acidic or basic) groups of the biosorbent and the chemical nature of the adsorbate have strong effect on the best pH for the biosorption studies. For

the removal of CV dye from aqueous solutions (50.0 mg L^{-1}) using ASP, the pH of the solution was varied from 2.0 to 10.0. For pH dependence studies, the removal of CV by ASP increases from 76.7% at pH 2.0 to $\approx 96\%$ within the range of pH 6.0 and 10.0. Therefore, the optimum pH region ranges from 6.0 to 10.0 for CV biosorption onto ASP. This observation is traceable to the pH$_{pzc}$ value of ASP. The pH$_{pzc}$ value of ASP is 6.40 (Fig. 6). A biosorbent with a lower pH value than pH$_{pzc}$ value will possess positively charged surface [15]. The CV dye possesses a positive charge in aqueous solutions even in a basic medium (see Fig. 1). Therefore, biosorption of CV dye will occur when the surface of the biosorbent is negatively charged. The electrostatic interactions of ASP occurred at pH > 6.40. For the rest of the experimental work, we fixed the pH of the CV solution at 7.0, which is

above the pH$_{PZC}$. This choice also took into consideration the neutrality of the wastewater effluents.

3.3. Kinetic studies and effect of contact time

The kinetic information of biosorption of CV dye onto ASP biosorbent was obtained using nonlinear pseudo-first-order, pseudo-second-order, and general-order kinetic models. Fig. 7(A) and (C) and Table 2 show the respective kinetic curves and the fitting parameters. The values of F_{error} were utilized to explain fitness of nonlinear kinetic models. F_{error} value is smaller if the theoretical q and experimental q values are closer [36,40] (see Eq. (5)). It is a fact that an increase in the number of parameters in nonlinear equations improves the tendency of the mathematical function to be better adjusted [39,50]. Therefore, it is necessary to check if the three-parameter kinetic model (general-order kinetic model) has advantages over the two-parameter kinetic models (pseudo-first-order and pseudo-second-order models). The number of fitting parameters (p term of Eq. (5)) was taken into account while computing F_{error}. For comparison, F_{error} value of each model was divided by F_{error} of the minimum value to obtain F_{error} ratio. General order kinetic model has F_{error} ratio value of 1.00. The F_{error} ratio values of the pseudo-first-order kinetic model vary from 7.59 to 8.57, while those of the pseudo-second-order model vary from 1.11 to 1.21. Based on F_{error} ratio values, the general-order kinetic model (lowest F_{error} ratio value of 1.00) gave the best fit of the kinetic data. The values F_{error} and F_{error} ratio are in agreement with the values of R^2_{adj}—an indication that the general-order kinetic model present the values closer to 1.

According to general-order kinetic model, the order of adsorption process must be of the same trend as that of a chemical reaction in which the order of reaction is determined experimentally [13,15,35,36,42,48,51] and not predetermined by a model. In this manuscript, the order (n) obtained for the kinetics at 50.0 and 100.0 mg L^{-1} are 2.131 and 2.100, respectively. Although several authors would consider the linear equations, a situation in which the kinetics of adsorption would follow the pseudo-second-order, which is a special case of general-order kinetic model [13,35,36,42,51]. However, it is preferable to determine the order experimentally instead of predetermine it before fitting the data.

Table 2 also presents another useful parameter, the half-life ($t_{1/2}$). Half-life is the time it takes to achieve 50% of q_e (amount adsorbed at the equilibrium). The values of $t_{1/2}$ were obtained by interpolation of the kinetic plots. Only $t_{1/2}$ values of general kinetic model are meaningful because the model gave the best fit of
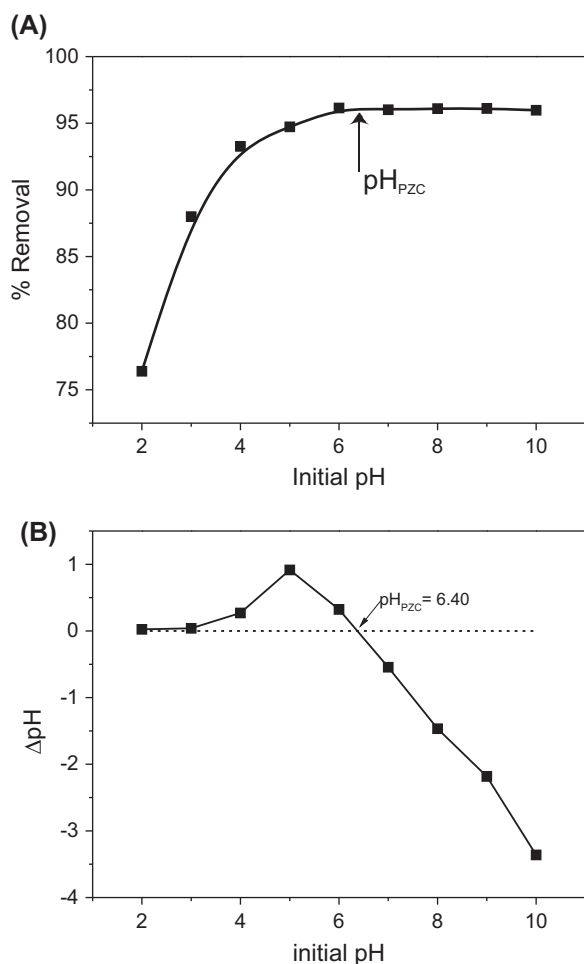

Fig. 6. Effect of pH on the biosorption of: (A) CV dye using ASP biosorbent and (B) pH$_{PZC}$ of ASP. Conditions: C_o, 50.0 mg L^{-1} of dye solution; the temperature, $25°C$; mass of biosorbent, 100.0 mg.
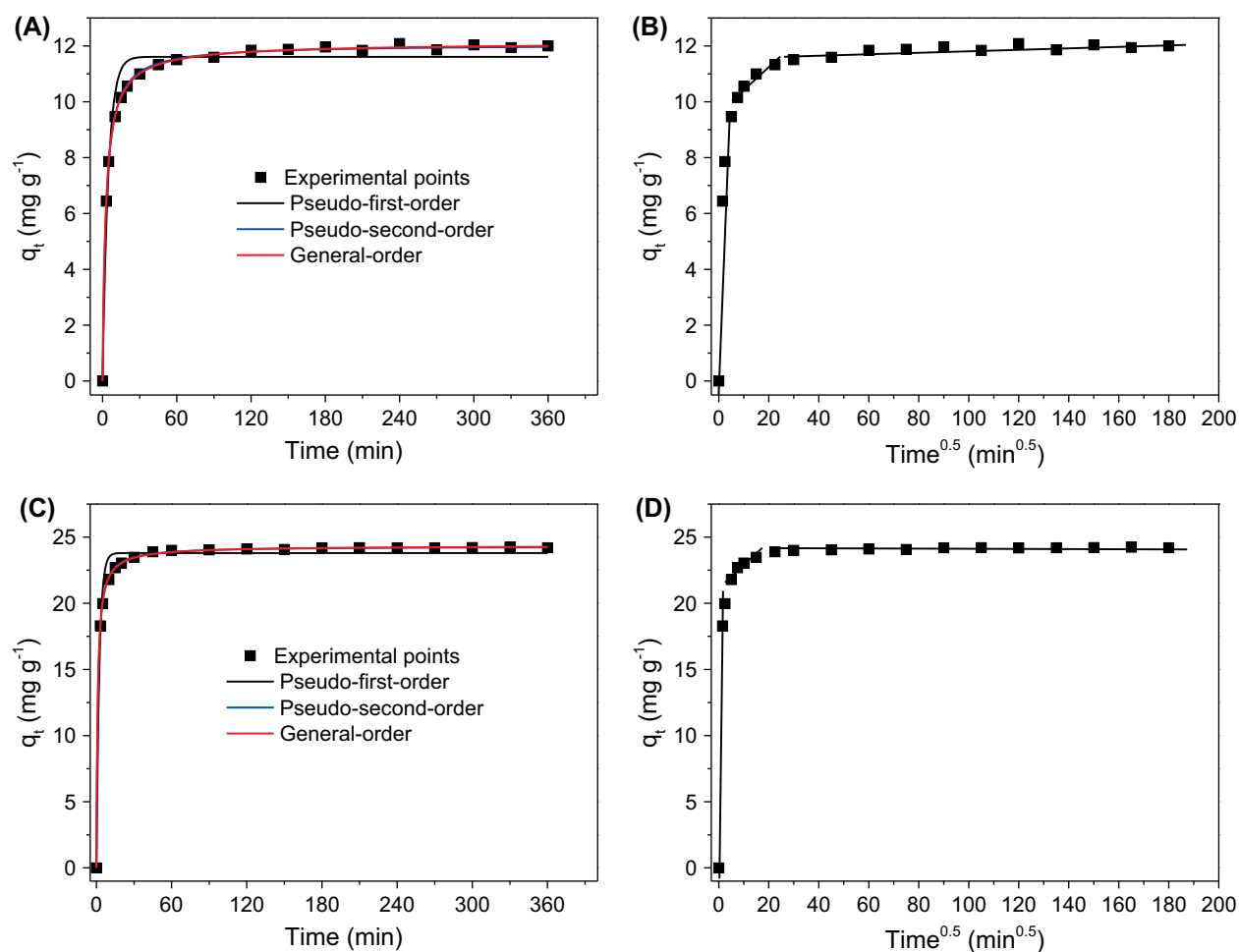
Fig. 7. (A) and (C) Kinetic biosorption curves of CV dye using ASP biosorbent. (B) and (D) Intra-particle diffusion plots of CV dye onto ASP biosorbent. (A) and (B) 50.0 mg L^{-1} CV; (C) and (D) 100.0 mg L^{-1}. Conditions: pH 7.0; biosorbent mass, 100.0 mg; and temperature, 25℃.

kinetic data. The kinetic of biosorption using 100.0 mg L^{-1} of CV is faster than that of 50.0 mg L^{-1} of the dye. This observation gives a piece of valuable information. It is an indication that the kinetics of biosorption of CV is controlled by diffusion, where the biosorption kinetics is faster at higher adsorbate concentrations [51].

The effect of mass transfer resistance on the binding of CV dye onto ASP was investigated using intraparticle diffusion model [42] (Table 2, Fig. 7(B) and (D)). The k_{id} (mg g^{-1} min$^{-0.5}$), the intraparticle diffusion constant, was obtained from the slope of the plot of q_t vs. $\sqrt{t}$.

The graph q_t vs. $\sqrt{t}$ for biosorption of CV onto ASP exhibited three linear regions. Each step is ascribed to each linear region of the plots (Fig. 7(B) and (D)). The first linear region, which is the fastest step, depicts the process by which dye molecules

diffuse into the surface of the biosorbents [42,48]. The second region, which is a delayed process, describes intraparticle diffusion [42,48]. The third region, which is obtained after equilibrium [42,48], designates diffusion through smaller pores. Considering that the three linear portions of these graphs play a role on the overall kinetics of adsorption, it could be concluded that the kinetic process depends on the film diffusion and the intraparticle diffusion.

From first data point of the third region, the minimum equilibrium time for biosorption of CV onto ASP is 60 min. Interpolation of the fitting curve (general order curve) gave 63.52 min as the time necessary to attain 95% of q_e at a 50.0 mg L^{-1} of CV solution. Contact time was taken as 90 min for other biosorption studies in this work. The contact time was elevated by 30 min to ensure that equilibrium is reached even at higher concentrations of CV dye [48].

Table 2
Kinetic parameters of CV dye biosorption onto ASP. Conditions: temperature, 25℃; pH 7.0; mass of biosorbent, 100.0 mg

	50.0 (mg L^{-1})	100.0 (mg L^{-1})
Pseudo-first-order		
k_1 (min^{-1})	0.2154	0.4298
q_e (mg g^{-1})	11.61	23.80
$t_{1/2}$ (min)	3.218	1.613
R^2_{adj}	0.9676	0.9843
F_{error} (mg g^{-1})	0.5307	0.6989
Pseudo-second-order		
k_2 (g mg^{-1} min^{-1})	0.03080	0.03982
q_e (mg g^{-1})	12.05	24.30
$t_{1/2}$ (min)	2.694	1.034
R^2_{adj}	0.9994	0.9997
F_{error} (mg g^{-1})	0.07472	0.1019
General-order		
k_N [h^{-1} (g mg^{-1})$^{n-1}$]	0.02365	0.03165
q_e (mg g^{-1})	12.14	24.37
n	2.131	2.100
$t_{1/2}$ (min)	2.641	0.9791
R^2_{adj}	0.9996	0.9997
F_{error} (mg g^{-1})	0.06196	0.09213
Intra-particle diffusion		
$k_{id,2}$ (mg g^{-1} min$^{-0.5}$)^a	0.07448	0.1573

^{a}Second stage.

3.4. Equilibrium studies

Adsorption isotherms explain the relationship between adsorption capacity (q_e) and adsorbate concentration (C_e) left in solution after attaining equilibrium at a fixed temperature. The parameters obtained from equilibrium models give valuable insights about the adsorption mechanism, the surface properties and adsorbent–adsorbate affinity. This study employed Langmuir [45], Freundlich [46], and Liu isotherms [47].

Adsorption isotherms were investigated between 15 and 55℃ using the following conditions: pH 7.0 of dye solution; biosorbent mass, 100.0 mg; contact time, 90 min. Fig. 8 shows the isotherm of CV onto ASP at 55℃; Table 3 shows the parameters. Using the F_{error} values shown in Table 3 the Liu model best described removal of CV by ASP between 15 and 55℃. Liu model has lowest F_{error} values—an indication that the theoretical q values of the isotherm model do not deviate much from the experimental q values.

F_{error} value of individual model was divided by the least F_{error} value to obtain F_{error} ratio, which was used to compare the fittingness of equilibrium isotherm models. Freundlich model gives F_{error} ratio values ranging from 10.03 to 18.79, while Langmuir model gives F_{error} values ranging from 7.00 to 7.71. Between 15 and 55℃, Liu model gave the F_{error} ratio of 1.00. On the basis of F_{error} ratio values, Liu isotherm model gives the best description of the isothermal data. Similarly, the analyses of F_{error} values and F_{error} ratio were in agreement with the values of R^2_{adj}, which means that these analyses help in choosing the best isotherm model.

The Liu isotherm model [47] is a combination of the Langmuir and Freundlich isotherm models; therefore, the monolayer assumption of Langmuir model is discarded and the infinite adsorption assumption that originates from the Freundlich model is not considered. The Liu model predicts that the active sites of the adsorbent cannot present the same energy. Therefore, the adsorbent may present active sites preferred by the adsorbate molecules for occupation [47]; however, saturation of the active sites should occur unlike in the Freundlich isotherm model. Taking into account that the biosorbent used in this study has different functional groups as shown by the FTIR spectrum (see Fig. 5); that the adsorbent texture is a fiber with roughness and it contains some spherical lignin-cellulosic material (see Fig. 4); and also that the material presents some mesopores and micropores (see Fig. 2), it is expected that the active sites of the biosorbent will not possess the same energy—the fact that is supported by the Liu isotherm model.

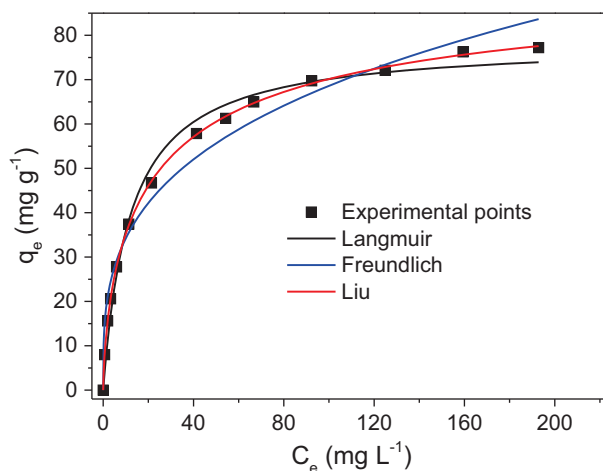The value of Q_{max}, maximum amount of CV dye removed at 55℃, is 95.98 mg g^{-1}. This Q_{max} value

Fig. 8. Isotherm of biosorption of CV dye onto ASP biosorbent at 55℃. Conditions: pH 7.0; ASP biosorbent mass, 100.0 mg; time of contact, 90 min.

Table 3
Isotherm parameters for CV biosorption using ASP. Conditions: pH 7.0; biosorbent mass, 100.0 mg; contact time, 90 min

	15℃	25℃	35℃	45℃	55℃
Langmuir					
Q_{max} (mg g^{-1})	75.19	77.85	78.39	80.15	78.50
K_L (L mg^{-1})	0.0950	0.08484	0.08003	0.07683	0.08379
R^2_{adj}	0.9927	0.9936	0.9919	0.9927	0.9871
F_{error} (mg g^{-1})	2.142	2.130	2.321	2.358	3.058
Freundlich					
K_F [mg g^{-1} (mg L^{-1})$^{-1/n_F}$]	18.60	17.51	18.17	16.36	17.08
n_F	3.606	3.398	3.463	3.186	3.311
R^2_{adj}	0.9566	0.9579	0.9630	0.9688	0.9734
F_{error} (mg g^{-1})	5.218	5.438	4.952	4.887	4.383
Liu					
Q_{max} (mg g^{-1})	83.88	86.89	89.72	92.93	95.98
K_g (L mg^{-1})	0.07023	0.06212	0.05559	0.04933	0.04442
n_L	0.7546	0.7671	0.7328	0.7349	0.6700
R^2_{adj}	0.9999	0.9999	0.9996	0.9999	0.9997
F_{error} (mg g^{-1})	0.2777	0.3097	0.5358	0.3269	0.4371

Table 4
Comparison of different adsorbents for the adsorption of CV dye

Adsorbent	Q_{max} (mg g^{-1})	Refs.
Pomegranate fruit shell powder	50.21	[21]
Formosa papaya seed powder	85.99	[22]
Jackfruit leaf powder	43.40	[33]
Jute fiber carbon	27.99	[52]
Rice husk activated carbon	11.18	[53]
Rice husk activated carbon	3.77	[53]
Eggshell	70.03	[54]
NaOH modified rice husk	44.88	[55]
Coir pith	65.53	[56]
Sawdust	37.83	[56]
Sugarcane fiber	10.44	[56]
Coniferous pinus bark powder	32.78	[57]
Peel of *Cucumis sativa* Fruit	34.24	[58]
Avocado seed powder	95.98	This work

could be considered very good for a biosorbent compared with other adsorbents reported in the literature [21,22,33,52–58]. A list of adsorbents reported [21,22,33,52–58] for removal of CV dye from aqueous solutions is presented in Table 4. ASP biosorbent presented highest sorption capacity out of the 14 adsorbents listed in Table 4.

3.5. Thermodynamics studies and mechanism of biosorption

Eqs. (22)–(24) were used to obtain the thermodynamic parameters. Gibb's free energy change

($\Delta G°$, kJ mol^{-1}), enthalpy change ($\Delta H°$, kJ mol^{-1}), and entropy change ($\Delta S°$, J mol^{-1} K^{-1}) were evaluated.

$$\Delta G° = \Delta H° - T\Delta S° \tag{22}$$

$$\Delta G° = -RT \ln(K) \tag{23}$$

Eq. (24) is obtained from Eqs. (22) and (23).

$$\ln(K) = \frac{\Delta S°}{R} - \frac{\Delta H°}{R} \times \frac{1}{T} \tag{24}$$

Table 5
Thermodynamic parameters of the adsorption of CV dye onto ASP biosorbent. Conditions: biosorbent mass, 100.0 mg; pH 7.0; contact time, 90 min

	Temperature (K)				
	288	298	308	318	328
K_g (L mol^{-1})	2.865×10^4	2.535×10^4	2.268×10^4	2.013×10^4	1.812×10^4
ΔG (kJ mol^{-1})	−24.57	−25.12	−25.68	−26.20	−26.74
$\Delta H°$ (kJ mol^{-1})	−9.01	–	–	–	–
$\Delta S°$ (J K^{-1} mol^{-1})	54.08	–	–	–	–
R_{adj}^2	0.9993	–	–	–	–
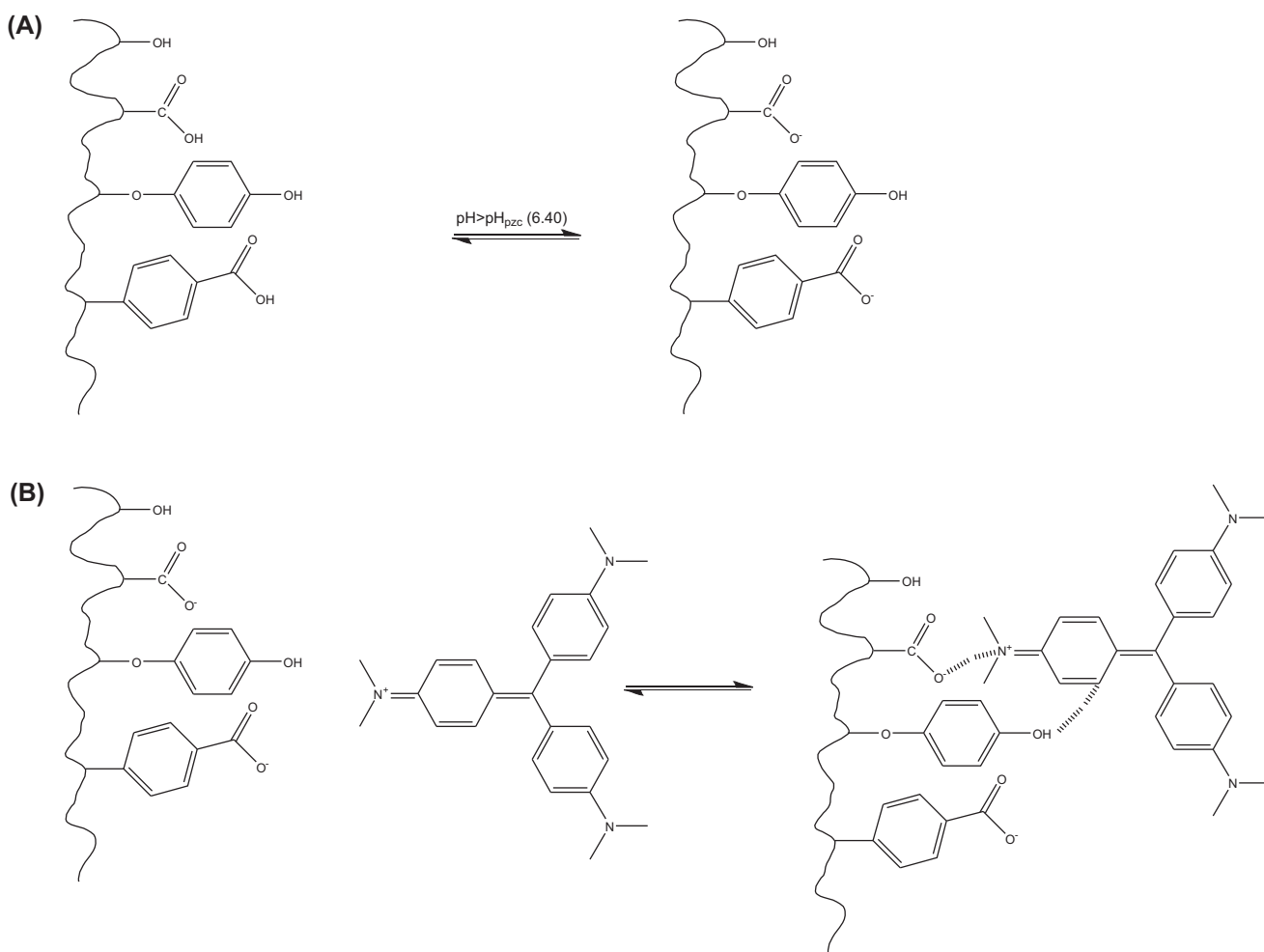
Fig. 9. (A) and (B) are the first and second steps of the mechanism of adsorption.

In Eqs. (22) and (23), R is the universal gas constant (8.314 J K^{-1} mol^{-1}); T is the absolute temperature (Kelvin); K is the biosorption equilibrium constant, which was obtained from the best isotherm fitting (K_g is the Liu equilibrium constant—which must be converted to SI unit using the molecular mass of the dye). By applying Eq. (24), enthalpy and entropy changes could be obtained from different
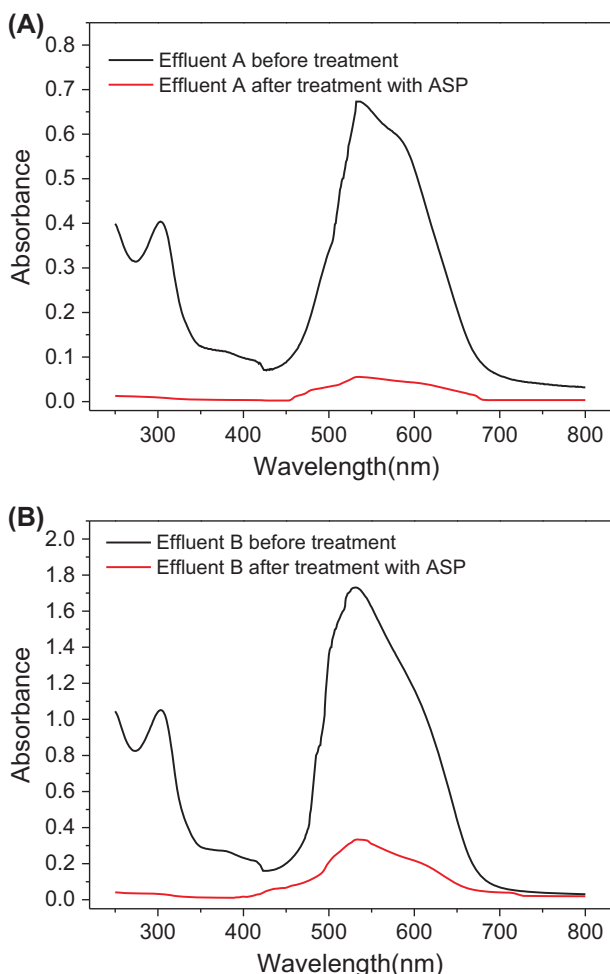
Fig. 10. UV–vis spectra of simulated dye effluents before and after treatment with ASP biosorbent. The temperature was fixed at 25℃. (A) Effluent *A* and (B) effluent *B*. For the composition of effluents, see Table 1.

equilibrium constants (different isotherm models) [13,15,16,19,20,35,36,41,42,48]. Also, the thermodynamic parameters can also be evaluated from the Liu equilibrium constant, K_g, as earlier reported [13,15,35,36,42,48].

The $\Delta H°$ value can be obtained from the slope of the linear plot of $\ln(K)$ vs. $1/T$, while $\Delta S°$ value is calculated from the intercept.

Table 5 presents the thermodynamic data. R^2_{adj} value of the linear fit is ≈1.0, which shows that the values of enthalpy and entropy obtained for the biosorbent are credible. The magnitude of enthalpy for CV removal by ASP corresponds to that of a physical adsorption [59]. The magnitude of enthalpy change is used to classify adsorbent–adsorbate interaction. Generally, physical sorption is less than 20 kJ mol^{-1} [59]. Negative value of $\Delta H°$ shows that the biosorption

process is exothermic. Negative value of $\Delta G°$ suggests that the biosorption process is feasible and favorable. Positive value of $\Delta S°$ indicates an increment in the randomness at the solid–liquid interface. The water-coordinated molecules are displaced by dye molecules hereby gain more translational entropy than what is lost by dye molecules, during biosorption, leading to an increase in the randomness of the adsorbent–adsorbate interaction [60,61].

On the basis of the data of pH studies, pH$_{pzc}$ (Fig. 6), characterization of the functional groups of ASP biosorbent (Fig. 5), kinetic studies (Table 2), equilibrium of biosorption (Table 3), and thermodynamic studies (Table 5) it is possible to establish a mechanism of biosorption of CV dye onto ASP biosorbent (see Fig. 9). The ASP biosorbent is a lignin-cellulosic material that presents these functional groups: aromatics, alcohols, ether, phenol, carboxylic acid, and aromatics [15]. At pH > pH$_{pzc}$ (pH > 6.40), the carboxylic groups of ASP biosorbent will be deprotonated (step 1 of the mechanism). When ASP biosorbent is in direct contact with CV dye, an electrostatic attraction of the cationic dye with the negative surface of the ASP biosorbent will occur [15]. These observations are in agreement with the data of pH dependence studies and pH$_{pzc}$ of ASP described above. In addition to this, van der Walls force between the aromatic groups of the CV dye and the aromatic groups of ASP biosorbent should be responsible for the biosorption mechanism, since the $\Delta H°$ of biosorption is −9.01 kJ mol^{-1}—the magnitude of enthalpy is consistent with physical adsorption (as described above).

3.6. Simulated dye-house effluents

The aim of this study is to evaluate the performance of ASP biosorbent in a medium containing mixtures of dyes and inorganic components—simulating a real dye-house effluent. In this work, two simulated dye-house effluents were utilized (see Table 1). Fig. 10 shows the spectra of the treated and untreated effluents, which were recorded from 250 to 800 nm on UV–vis spectrophotometer. In order to evaluate the percentage of removal of the mixture of dyes, the areas under the absorption bands were measured. The ratio of the areas (the area of the absorption bands of the effluent after the treatment with ASP biosorbent was divided by the area of the absorption band of the effluent before the treatment) multiplied by 100 gave the percentage of the dyes mixture removed from the simulated effluents. The percentages of removal of a mixture of dyes using ASP are 92.9% (effluent *A*) and 84.4% (effluent *B*). ASP shows

good result for the treatment of dye-rich wastewater and decreases severity of a real wastewater effluent, when these data are compared with published work [1,13,15,20,35,36,42,48].

4. Conclusion

ASP was utilized in this work for removal of CV dye from aqueous solutions. Influences of initial pH of solution, contact time, initial dye concentration, and temperature were investigated. The usability of ASP for simulated-effluents treatment was also investigated. The FTIR data of ASP showed that carboxyl group, hydroxyl group, and aromatics are responsible for removal of CV dye. Higher biosorption capacities of CV onto ASP were observed between pH 6.0 and 10.0. Using 100 mg of ASP/25.0 mL of CV, the equilibrium time was achieved in 90 min. The sorption kinetics of CV onto ASP was best described by general-order kinetic model. For isothermal study, the Liu isotherm model was the best model that explained the biosorption of CV dye onto ASP biosorbent. On the basis of the parameters from Liu isotherm model, the maximum adsorption capacity was 95.98 mg g^{-1} at 55℃. ASP removed 92.9 and 84.4% of simulated textile effluents *A* and *B*, respectively. These results imply that ASP can be utilized as biosorbent for the treatment of wastewaters.

References

[1] L.D.T. Prola, E. Acayanka, E.C. Lima, C. Bestetti, W.O. Santos, F.A. Pavan, S.L.P. Dias, C.R.T. Tarley, Application of aqai stalks as biosorbent for the removal of Evans Blue and Vilmafix Red RR-2B dyes from aqueous solutions, Desalin. Water Treat. 51 (2013) 4582–4592.

[2] B. Royer, N.F. Cardoso, E.C. Lima, V.S.O. Ruiz, T.R. Macedo, C. Airoldi, Organofunctionalized kenyaite for dye removal from aqueous solution, J. Colloid Interface Sci. 336 (2009) 398–405.

[3] L.G. da Silva, R. Ruggiero, P.M. Gontijo, R.B. Pinto, B. Royer, E.C. Lima, T.H.M. Fernandes, T. Calvete, Adsorption of Brilliant Red 2BE dye from water solutions by a chemically modified sugarcane bagasse lignin, Chem. Eng. J. 168 (2011) 620–628.

[4] S. Gupte, H. Keharia, A. Gupte, Toxicity analysis of azo Red BS and Methyl Red dye solutions on earthworm (*Pheretima phosthuma*), micro-organisms, and plants, Desalin. Water Treat. 51 (2013) 4556–4565.

[5] N.M. Mahmoodi, S. Khorramfar, Degradation of dyes using combined photo-Fenton/activated carbon: Synergistic effect, Desalin. Water Treat. 52 (2014) 5007–5014.

[6] P.A. Carneiro, G.A. Umbuzeiro, D.P. Oliveira, M.V.B. Zanoni, Assessment of water contamination caused by a mutagenic textile effluent/dyehouse effluent bearing disperse dyes, J. Hazard. Mater. 174 (2010) 694–699.

[7] M. Oplatowska, R.F. Donnelly, R.J. Majithiya, D.G. Glenn Kennedy, C.T. Elliott, The potential for human exposure, direct and indirect, to the suspected carcinogenic triphenylmethane dye Brilliant Green from green paper towels, Food Chem. Toxicol. 49 (2011) 1870–1876.

[8] S. Danwittayakul, M. Jaisai, J. Dutta, Efficient solar photocatalytic degradation of textile wastewater using ZnO/ZTO composites, Appl. Catal. B: Environ. 163 (2015) 1–8.

[9] E.J.R. Almeida, C.R. Corso, Comparative study of toxicity of azo dye Procion Red MX-5B following biosorption and biodegradation treatments with the fungi *Aspergillus niger* and *Aspergillus terreus*, Chemosphere 112 (2014) 317–322.

[10] G.G. Bessegato, J.C. Cardoso, M.V.B. Zanoni, Enhanced photoelectrocatalytic degradation of an acid dye with boron-doped TiO₂ nanotube anodes, Catal. Today, 240, Part A (2015) 100–106.

[11] G. Muthuraman, Extractive removal of astacryl blue BG and astacryl golden yellow dyes from aqueous solutions by liquid–liquid extraction, Desalination 277 (2011) 308–312.

[12] L. Doumic, G. Salierno, M. Cassanello, P. Haure, M. Ayude, Efficient removal of Orange G using Prussian Blue nanoparticles supported over alumina, Catal. Today 240 (2015) 67–72.

[13] M.A. Adebayo, L.D.T. Prola, E.C. Lima, M.J. Puchana-Rosero, R. Cataluña, C. Saucier, C.S. Umpierres, J.C.P. Vaghetti, L.G. da Silva, R. Ruggiero, Adsorption of Procion Blue MX-R dye from aqueous solutions by lignin chemically modified with aluminium and manganese, J. Hazard. Mater. 268 (2014) 43–50.

[14] B. Royer, N.F. Cardoso, E.C. Lima, T.R. Macedo, C. Airoldi, A useful organofunctionalized layered silicate for textile dye removal, J. Hazard. Mater. 181 (2010) 366–374.

[15] L.D.T. Prola, E. Acayanka, E.C. Lima, C.S. Umpierres, J.C.P. Vaghetti, W.O. Santos, S. Laminsi, P.T. Djifon, Comparison of *Jatropha curcas* shells in natural form and treated by non-thermal plasma as biosorbents for removal of Reactive Red 120 textile dye from aqueous solution, Ind. Crop. Prod. 46 (2013) 328–340.

[16] G.L. Dotto, E.C. Lima, L.A.A. Pinto, Biosorption of food dyes onto *Spirulina platensis* nanoparticles: Equilibrium isotherm and thermodynamic analysis, Bioresour. Technol. 103 (2012) 123–130.

[17] M.E. Fernandez, G.V. Nunell, P.R. Bonelli, A.L. Cukierman, Activated carbon developed from orange peels: Batch and dynamic competitive adsorption of basic dyes, Ind. Crops Prod. 62 (2014) 437–445.

[18] O. Pezoti, A.L. Cazetta, I.P.A.F. Souza, K.C. Bedin, A.C. Martins, T.L. Silva, V.C. Almeida, Adsorption studies of methylene blue onto $ZnCl_2$-activated carbon produced from buriti shells (*Mauritia flexuosa* L.), J. Ind. Eng. Chem. 20 (2014) 4401–4407.

[19] T. Calvete, E.C. Lima, N.F. Cardoso, J.C.P. Vaghetti, S.L.P. Dias, F.A. Pavan, Application of carbon adsorbents prepared from Brazilian-pine fruit shell for the removal of reactive orange 16 from aqueous solution: Kinetic, equilibrium, and thermodynamic studies, J. Environ. Manage. 91 (2010) 1695–1706.

[20] N.F. Cardoso, R.B. Pinto, E.C. Lima, T. Calvete, C.V. Amavisca, B. Royer, M.L. Cunha, T.H.M. Fernandes, I.S. Pinto, Removal of remazol black B textile dye from aqueous solution by adsorption, Desalination 269 (2011) 92–103.

[21] M.B. Silveira, F.A. Pavan, N.F. Gelos, E.C. Lima, S.L.P. Dias, Punica granatum Shell Preparation, Characterization, and use for crystal violet removal from aqueous solution, Clean—Soil, Air, Water 42 (2014) 939–946.

[22] F.A. Pavan, E.S. Camacho, E.C. Lima, G.L. Dotto, V.T.A. Branco, S.L.P. Dias, Formosa papaya seed powder (FPSP): Preparation, characterization and application as an alternative adsorbent for the removal of crystal violet from aqueous phase, J. Environ. Chem. Eng. 2 (2014) 230–238.

[23] M.P. Elizalde-González, J. Mattusch, A.A. Peláez-Cid, R. Wennrich, Characterization of adsorbent materials prepared from avocado kernel seeds: Natural, activated and carbonized forms, J. Anal. Appl. Pyrol. 78 (2007) 185–193.

[24] Situação Atual e Perspectivas da Cadeia Produtiva do Abacate no Brasil, Casa do Produtor Rural Esalq/USP (Current situation and prospects of the production chain Avocado in Brazil, House of Rural Producer Esalq/USP). Available from: <http://www.esalq.usp.br/cprural/artigos.php?col_id=32> website viewed at November 25th, 2014.

[25] A.M. Aljeboree, A.F. Alkaim, A.H. Al-Dujaili, Adsorption isotherm, kinetic modeling and thermodynamics of crystal violet dye on coconut husk-based activated carbon, Desalin. Water Treat. 53 (2015) 3656–3667.

[26] S. Kaur, S. Rani, R.K. Mahajan, Adsorption of dye crystal violet onto surface-modified *Eichhornia crassipes*, Desalin. Water Treat. 53 (2015) 1957–1969.

[27] K. Vijayaraghavan, Y. Premkumar, J. Jegan, Malachite green and crystal violet biosorption onto coco-peat: Characterization and removal studies, Desalin. Water Treat. (in press), doi: 10.1080/19443994.2015.1011709.

[28] E. Bağda, The feasibility of using *Rosa canina* galls as an effective new biosorbent for removal of methylene blue and crystal violet, Desalin. Water Treat. 43 (2012) 63–75.

[29] I.A.W. Tan, B.H. Hameed, Removal of crystal violet dye from aqueous solutions using rubber (*Hevea brasillensis*) seed shell-based biosorbent, Desalin. Water Treat. 48 (2012) 174–181.

[30] X. Ren, W. Xiao, R. Zhang, Y. Shang, R. Han, Adsorption of crystal violet from aqueous solution by chemically modified phoenix tree leaves in batch mode, Desalin. Water Treat. 53 (2015) 1324–1334.

[31] B.K. Suyamboo, R. Srikrishnaperumal, Biosorption of crystal violet onto *cyperus rotundus* in batch system: Kinetic and equilibrium modeling, Desalin. Water Treat. 52 (2014) 3535–3546.

[32] S. Kaur, S. Rani, R.K. Mahajan, Adsorptive removal of dye crystal violet onto low-cost carbon produced from Eichhornia plant: Kinetic, equilibrium, and thermodynamic studies, Desalin. Water Treat. 53 (2015) 543–556.

[33] P.D. Saha, S. Chakraborty, S. Chowdhury, Batch and continuous (fixed-bed column) biosorption of crystal violet by *Artocarpus heterophyllus* (jackfruit) leaf powder, Colloids Surf., B 92 (2012) 262–270.

[34] L. Zhang, H. Zhang, W. Guo, Y. Tian, Removal of malachite green and crystal violet cationic dyes from aqueous solution using activated sintering process red mud, Appl. Clay Sci. 93–94 (2014) 85–93.

[35] D.C. dos Santos, M.A. Adebayo, S.F.P. de Fátima Pinheiro Pereira, L.D.T. Prola, R. Cataluña, E.C. Lima, C. Saucier, C.R. Gally, F.M. Machado, New carbon composite adsorbents for the removal of textile dyes from aqueous solutions: Kinetic, equilibrium, and thermodynamic studies, Korean J. Chem. Eng. 31 (2014) 1470–1479.

[36] M.C. Ribas, M.A. Adebayo, L.D.T. Prola, E.C. Lima, R. Cataluña, L.A. Feris, M.J. Puchana-Rosero, F.M. Machado, F.A. Pavan, T. Calvete, Comparison of a homemade cocoa shell activated carbon with commercial activated carbon for the removal of reactive violet 5 dye from aqueous solutions, Chem. Eng. J. 248 (2014) 315–326.

[37] E.C. Lima, F.J. Krug, J.A. Nóbrega, A.R.A. Nogueira, Determination of ytterbium in animal faeces by tungsten coil electrothermal atomic absorption spectrometry, Talanta 47 (1998) 613–623.

[38] E.C. Lima, P.G. Fenga, J.R. Romero, W.F. de Giovani, Electrochemical behavior of $[Ru(4,4´-Me_2bpy)_2(PPh_3)(H_2O)](ClO_4)_2$ in homogeneous solution and incorporated into carbon paste electrodes. Application to oxidation of benzylic compounds, Polyhedron 17 (1998) 313–318.

[39] D.L. Massart, B.G.M. Vandeginste, L.M.C. Buydens, S. De Jong, P.J. Lewi, J. Smeyers-Verbeke, Handbook of Chemometrics and Qualimetrics, Part A, Elsevier, Amsterdam, 1997.

[40] K. Vasanth Kumar, K. Porkodi, F. Rocha, Comparison of various error functions in predicting the optimum isotherm by linear and non-linear regression analysis for the sorption of basic red 9 by activated carbon, J. Hazard. Mater. 150 (2008) 158–165.

[41] Y. Liu, Y.J. Liu, Biosorption isotherms, kinetics and thermodynamics, Sep. Purif. Technol. 61 (2008) 229–242.

[42] W.S. Alencar, E.C. Lima, B. Royer, B.D. dos Santos, T. Calvete, E.A. da Silva, C.N. Alves, Application of aqai stalks as biosorbents for the removal of the dye Procion Blue MX-R from aqueous solution, Sep. Sci. Technol. 47 (2012) 513–526.

[43] Y.S. Ho, Review of second-order models for adsorption systems, J. Hazard. Mater. 136 (2006) 681–689.

[44] W.J. Weber Jr., J.C. Morris, Kinetics of adsorption on carbon from solution, J. Sanit. Eng. Div. Am. Soc. Civil Eng. 89 (1963) 31–59.

[45] I. Langmuir, The adsorption of gases on plane surfaces of glass, mica and platinum, J. Am. Chem. Soc. 40 (1918) 1361–1403.

[46] H. Freundlich, Adsorption in solution, Phys. Chem. Soc. 40 (1906) 1361–1368.

[47] Y. Liu, H. Xu, S.F. Yang, J.H. Tay, A general model for biosorption of Cd^{2+}, Cu^{2+} and Zn^{2+} by aerobic granules, J. Biotechnol. 102 (2003) 233–239.

[48] L.D.T. Prola, F.M. Machado, C.P. Bergmann, F.E. de Souza, C.R. Gally, E.C. Lima, M.A. Adebayo, S.L.P. Dias, T. Calvete, Adsorption of Direct Blue 53 dye from aqueous solutions by multi-walled carbon nanotubes and activated carbon, J. Environ. Manage. 130 (2013) 166–175.

[49] J. Gregg, K.S.W. Sing, Adsorption, Surface Area and Porosity, Academic Press, London, 1982 (Chapters 3 and 4).

[50] R.E. Bruns, I.S. Scarmino, B. de Barros Neto, Statistical Design-Chemometrics, first ed., Elsevier, Amsterdam, 2006.

[51] O. Levenspiel, Chemical Reaction Engineering, third ed., John Wiley & Sons, New York, NY, 1999.

[52] K. Porkodi, K. Vasanth Kumar, Equilibrium, kinetics and mechanism modeling and simulation of basic and acid dyes sorption onto jute fiber carbon: Eosin yellow, malachite green and crystal violet single component systems, J. Hazard. Mater. 143 (2007) 311–327.

[53] K. Mohanty, J.T. Naidu, B.C. Meikap, M.N. Biswas, Removal of crystal violet from wastewater by activated carbons prepared from rice husk, Ind. Eng. Chem. Res. 45 (2006) 5165–5171.

[54] S. Chowdhury, S. Chakraborty, P.D. Saha, Removal of crystal violet from aqueous solution by adsorption onto eggshells: Equilibrium, kinetics, Thermodynamics and artificial neural network modeling, Waste Biomass Valor 4 (2013) 655–664.

[55] S. Chakraborty, S. Chowdhury, P.D. Das Saha, Adsorption of crystal violet from aqueous solution onto NaOH-modified rice husk, Carbohydr. Polym. 86 (2011) 1533–1541.

[56] H. Parab, M. Sudersanan, N. Shenoy, T. Pathare, B. Vaze, Use of agro-industrial wastes for removal of basic dyes from aqueous solutions, Clean—Soil, Air, Water 37 (2009) 963–969.

[57] R. Ahmad, Studies on adsorption of crystal violet dye from aqueous solution onto coniferous pinus bark powder (CPBP), J. Hazard. Mater. 171 (2009) 767–773.

[58] T. Smitha, S. Thirumalisamy, S. Manonmani, Equilibrium and kinetics study of adsorption of crystal violet onto the peel of *Cucumis sativa* fruit from aqueous solution, E-J. Chem. 9 (2012) 1091–1101.

[59] C.L. Sun, C.S. Wang, Estimation on the intramolecular hydrogen-bonding energies in proteins and peptides by the analytic potential energy function, J. Mol. Struct. 956 (2010) 38–43.

[60] G.Z. Kyzas, N.K. Lazaridis, D.N. Bikiaris, Optimization of chitosan and β-cyclodextrin molecularly imprinted polymer synthesis for dye adsorption, Carbohyd. Polym. 91 (2013) 198–208.

[61] N.A. Travlou, G.Z. Kyzas, N.K. Lazaridis, E.A. Deliyanni, Graphite oxide/chitosan composite for reactive dye removal, Chem. Eng. J. 217 (2013) 256–265.